Journal of Applied Pharmaceutical Science 2025. Article in Press
Available online at http://www.japsonline.com
DOI: 10.7324/JAPS.2026.251960
ISSN 2231-3354

Effects of polyphenolic extracts from Mediterranean forage crops on cholinesterases and amyloid aggregation relevant to neurodegenerative diseases

Antonio D'Errico[1], Pierluigi Reveglia[2], Rosarita Nasso[1], Alessandro Maugeri[3], Mariorosario Masullo[1*], Rosaria Arcone[1], Lucia Lecce[2], Emmanuele De Vendittis[4], Rosario Rullo[5]

[1]Department of Medical, Movement and Well-Being Sciences, University of Naples "Parthenope", Napoli, Italy.
[2]Department of Clinical and Experimental Medicine, University of Foggia, Foggia, Italy.
[3]Department of Veterinary Sciences, University of Messina, Messina, Italy.
[4]Department of Molecular Medicine and Medical Biotechnologies, University of Naples Federico II, Napoli, Italy.
[5]Institute for the Animal Production Systems in the Mediterranean Environment, Consiglio Nazionale delle Ricerche, Portici, Italy.

ARTICLE HISTORY

Received on: 10/04/2025
Accepted on: 13/09/2025
Available Online: XX

Key words:
Mediterranean forage crops, polyphenols, LC-MS/MS, MRM analysis, cholinesterases, amyloidogenesis, neuroblastoma cancer cells.

ABSTRACT

Alzheimer's and Parkinson's diseases are the most common neurodegenerative disorders of the central nervous system, characterized by progressive neuronal death and neurological dysfunction. There is currently no treatment that effectively slows the disease progression, and the synthetic drugs proposed to alleviate the symptoms often cause side effects. Many studies are now focused on neuroprotective properties exhibited by natural agents, such as polyphenols, whose action on different cell signaling pathways is well known. In this article, we analyzed the composition and the properties of polyphenolic extracts from forage plants, such as *Lotus ornithopodioides*, *Hedysarum coronarium*, *Medicago sativa*, and *Cichorium intybus*. The liquid chromatography-mass spectrometry/mass spectrometry analysis on the extracts allowed the identification of total 24 phenolic acids and 25 flavonoids. The effects of the extracts on key enzymes of cholinergic neurotransmission, such as acetyl cholinesterase and butyryl cholinesterase, were examined, together with an investigation on the aggregation and disaggregation of amyloid fibrils. The polyphenols acted as inhibitors of the considered enzymes and interfered with the amyloidogenesis process, with differences depending on the specific extracts. The inhibition constants towards cholinesterases ranged in the 60–240 μM interval; the extracts showed different inhibition mechanisms, from competitive to non-competitive. Differences also emerged in the amyloidogenesis process, with IC_{50} values comprised in a large interval. Finally, the extract from *M. sativa* significantly reduced the cell viability of the human neuroblastoma cell line SH-SY5Y. These results suggest that polyphenols extracted from these plants may behave as multitargeting agents against key factors of Alzheimer's and Parkinson's diseases. Therefore, they can be considered as promising candidates for the prevention and management of symptoms of these neurodegenerative disorders in combination with pharmacological therapies.

1. INTRODUCTION

In elderly people, increased life expectancy is frequently accompanied by the appearance of neurodegenerative disorders of the central nervous system, such as Alzheimer's disease (AD) and Parkinson's disease (PD) [1,2]. These pathologies, characterized by a progressive neuronal death, cause severe disabilities, such as memory loss, aphasia, disorientation, depression, tremor, limb rigidity, slowness, walking difficulties, and so on [3]. Furthermore, worsening of these disabilities with age, and the need for long periods for care and therapy, entail high costs even for families of patients affected by these pathologies [4]. AD and PD are the consequence of multifactorial disorders,

*Corresponding Author
Mariorosario Masullo, Department of Medical, Movement and Well-Being Sciences, University of Naples "Parthenope", Napoli, Italy.
E-mail: mario.masullo @ uniparthenope.it

which alter the neurotransmission metabolism and induce the formation of protein aggregates [5,6]. The multifactorial nature of these disorders may explain a missing effective and novel therapeutic treatment, capable to prevent, delay and counteract the progression of these diseases [7].

Among enzymes involved in these multifactorial disorders, a central role is played by enzymes involved in the cholinergic neurotransmission, such as acetylcholinesterase (AChE) and butyrylcholinesterase (BuChE) [8,9]. Indeed, these enzymes are primarily responsible for the hydrolysis of acetylcholine or butyrylcholine, respectively, thus allowing the return of the activated cholinergic neuron to its resting state [10]. Therefore, AChE and BuChE inhibition by synthetic or natural compounds has relevant implications for the onset of neurodegenerative disorders [7,11,12]. In addition, AChE is also implicated in the aggregation of amyloid-beta (Aβ) peptides leading to the abnormal formation of Aβ plaques around neurons, a hallmark of AD [13]. Therefore, the identification of natural inhibitors of the filamentous aggregation of Aβ peptides would be extremely interesting for a novel therapeutic approach to this neurodegenerative disorder [11,14].

Therapies for AD and PD treatment are primarily based on cholinesterase inhibitors, and the most common synthetic drugs, such as donepezil, galantamine, and rivastigmine, are used against these disorders, although their usage is often accompanied by bothersome side effects, such as loss of appetite, hepatotoxicity, and gastrointestinal disorders [15]. To overcome this problem, novel research is focused on the identification of plant-derived natural agents, endowed with neuroprotective properties acting with multi-targeting effects [16–18]. Under these concerns, polyphenols extracted from plants have shown several interesting properties, such as the decrease in the incidence of neurodegenerative diseases, because acting on different cell signaling pathways [19–21]. In particular, flavonoid-rich extracts from Mediterranean plants can modulate AChE and BuChE activity, such as those from Annurca apple flash [18] and lemon peel [22]. In addition, tannins derived from Mediterranean plants have also demonstrated inhibitory activity on AChE and BuChE [23,24]. Flavonoids and tannins, exerting beneficial effects on human health, are present also in plants used as forage crops [25] belonging to the Fabaceae family [26], such as *Lotus ornithopodioides* (known as Southern Bird's-foot trefoil), *Hedysarum coronarium* (Sulla) [27], *Medicago sativa* (Alfalfa) [28,29], as well as in *Cichorium intybus L.* (Chicory) belonging to the Asteraceae family. All these abundant and edible plants, used in diet and medicine for their strong antioxidant, anti-inflammatory, and antimicrobial properties [30,31], represent a suitable source to produce phytochemicals and products for healthcare and treatment of various disorders.

In a recent article, we have described the antioxidant properties of polyphenol- or tannin-enriched extracts from leaves of *L. ornithopodioides*, *H. coronarium*, *M. sativa*, and *C. intybus* [32]. Now, in this study, we focused our attention on the chemical characterization of these extracts and their anticholinesterase activity. To this aim, we determined the effect of these extracts on AChE and BuChE activity, because these enzymes are the major targets for developing new molecules for AD and PD treatment. In addition, the ability of these extracts either to reduce or revert the peptide $A\beta_{1-40}$ self-aggregation was carried out by *in vitro* assays. Finally, in light of potential therapeutic applications of these extracts in the prevention, delay, and management of AD and PD, we also performed preliminary evaluations of their cytotoxic effect, using *in vitro* cellular models consisting of human neuroblastoma SH-SY5Y cell line. The results of this investigation show that a natural extract from *M. sativa* may be useful as a possible co-adjutant to a therapeutic approach to AD and PD.

2. MATERIALS AND METHODS

2.1. Materials and standards

The following reagents methanol (MeOH), formic acid, and quinaldic acid, were liquid chromatography-mass spectrometry (LC-MS) grade and purchased from Sigma Aldrich (Darmstadt, Germany). The Phenolic Acids and Alcohols Standard Mixture-V2 along with the Flavonoids Standard Mixture-V2 were obtained from MetaSci library (https://www.metasci.ca/). These substances were used for peak identification, Multiple Reaction Monitoring (MRM) method development, and calibration curves. Acetylthiocholine, butyrylthiocholine, 5',5'-dithiobis-2-nitrobenzoic (DTNB), thioflavine T, and the enzymes AChE and BuChE, were acquired from Sigma-Aldrich (Milano, Italy). The human β-amyloid peptide (1–40, cat. ab120479) was obtained from Abcam (Cambridge, UK). All other reagents were analytical grade.

2.2. Methods

2.2.1. LC-MS/MS analysis of phenolic acids and flavonoids

Plants of Mediterranean forage crops considered in this study were *Lotus ornithopodioides*, *Hedysarum coronarium*, *M. sativa*, and *C. intybus*. The origin of these plants and preparation of the relative extracts were extensively reported in our previous work [32]. In particular, extracts from *L. ornithopodioides* and *H. coronarium*, enriched in condensed tannins, were indicated as *Lo*CT and *Hc*CT, respectively, whereas extracts from *M. sativa* and *C. intybus*, enriched in flavonoids, were indicated as *Ms*F and *Ci*F, respectively. The lyophilized material obtained from these extracts was dissolved in dimethylsulfoxide (DMSO), and the different groups of phenolic compounds, such as total phenolics, flavonoids, and proanthocyanidins, were determined as previously reported [32]. Total phenolics, measured as gallic acid equivalents, were used for a comparative evaluation of polyphenols among extracts.

The LC-MS/MS system used for the analysis of the extracts included a UHPLC (Nexera Series LC-40, Shimadzu, Kyoto, Japan) coupled to a triple quadrupole/linear ion trap tandem mass spectrometer (QTRAP 4500, AB Sciex, Framingham, MA, USA) that was equipped with a Turbo V ion source. Instrument control, data acquisition, and processing were achieved by the associated Analyst 1.6 and Multiquant 3.0 software. Quantification of phenolic acids and flavonoids was conducted in the same conditions as previously reported [33]. The Q1 mass, the Q3 transition, the best parameters, and retention times are described in the Supplementary Table S1.

Chromatograms for both phenolic acids and flavonoids are reported as Supplementary Figures S1 and S2.

Validation of chromatographic methods was conducted by analyzing calibration curves. Limits of detection and quantification are reported in Supplementary Table S2.

2.2.2. Cholinesterase assay and related kinetic parameters

The activity of AChE and BuChE was determined by Ellman's method [34], as previously reported [35], using acetylthiocholine or butyrylthiocholine as substrates, respectively. The reaction mixture contained 330 µM DTNB, 500 µM acetylthiocholine or butyrylthiocholine, respectively, and increasing concentrations of the extracts in a 500-µl final volume of 0.1 M sodium phosphate buffer, pH 7.4. The reaction started with the addition of 100 mU/ml AChE or BuChE, and the absorbance increase at 412 nm was followed kinetically, employing a Cary 100 UV–VIS Spectrophotometer (Agilent, Santa Clara, CA, USA). The steady-state enzymatic activity was derived from the initial rate of reaction obtained from the linear part of the kinetics. The inhibitor concentration required to cause a 50% reduction of enzymatic activity (IC_{50}) was derived from semi-logarithmic plots, in which the logarithm of the residual activity ratio was plotted against the extract concentration; the IC_{50} value was extrapolated from the slope of the resulting straight lines [35].

The kinetic parameters K_M and V_{max} of AChE and BuChE activity were determined as previously described [11], by measuring the initial velocity (v_i) of the reaction at different concentrations of the specific thiolated substrate. Values of the inhibition constant (K_i) and the putative mechanism of inhibition were derived by comparing the above-mentioned kinetic parameters in the absence or in the presence of fixed concentrations of the extracts, using the following equations for competitive (a), noncompetitive (b), or uncompetitive (c) mechanism:

$$K_i = K_M \times [I]/(K'_M - K_M) \quad \text{equation (a)}$$

$$K_i = V'_{max} \times [I]/(V_{max} - V'_{max}) \quad \text{equation (b)}$$

$$K_i = V'_{max} \times [I]/(V_{max} - V'_{max}) \text{ and}$$

$$K_i = K'_M \times [I]/(K_M - K'_M) \quad \text{equations (c)}$$

where K'_M or V'_{max} represent the K_M or V_{max} measured in the presence of inhibitor concentration [I].

2.2.3. Assay for self-aggregation or disaggregation of Aβ$_{1–40}$ fibrils

Self-aggregation of $A\beta_{1–40}$ fibrils was achieved as previously reported [11], by incubating for 24 hours at 4°C a 12-µl reaction mixture of aggregation buffer, containing 200 mM sodium phosphate buffer, pH 8.0, and 0.5% (v/v) DMSO, in which 96 µM $A\beta_{1–40}$ peptide was dissolved. The reaction ended by adding 0.5 ml of 1.6 µM thioflavine T in 50 mM glycine-NaOH buffer, pH 8.5, and the fluorescence intensity was monitored for 5 minutes at 25°C, using a Cary Eclipse Spectrofluorimeter (Agilent, Santa Clara, CA, USA). Excitation and emission wavelengths were set at 446 and 490 nm, respectively, and excitation and emission beam slits were both set at 10 nm. The fluorescence value at the plateau was averaged over a scan of at least 2 minutes, and the fluorescence background due to extracts and other components in the reaction mixture was subtracted. To determine the inhibition ratio in the self-aggregation reaction, the decrease of fluorescence signal observed in the presence of various concentrations of extracts was compared to that measured in their absence. The concentration leading to 50% residual $A\beta_{1–40}$ self-aggregation (IC_{50}) was derived from a semi logarithmic plot in which the logarithm of the residual activity ratio was plotted against the extract concentration.

The assay for disaggregation of $A\beta_{1–40}$ fibrils entailed a previous fibril aggregation step as reported above. Then, the extent of fibril disaggregation caused by extracts was evaluated by incubating for additional 24 hours at 4°C a reaction mixture containing 12 µl of the formed fibril mixture with 2 µl of aggregation buffer, without or with various concentrations of the extracts. The disaggregation ended with the addition of 0.5 ml of the thioflavine T solution, and the fluorescence was measured as reported above. The concentration of extract leading to 50% residual Aβ fibrils disaggregation (IC_{50}) was derived from a semi logarithmic plot, in which the logarithm of the residual activity ratio was plotted against the extract concentration.

2.3. Cell cultures and treatments

The human neuroblastoma SH-SY5Y cell line (American Type Culture Collection, Manassas, VA, USA) was maintained in Dulbecco's modified Eagle medium (DMEM; Microgem Laboratory Research, Milan, Italy), containing 10% heat-inactivated fetal bovine serum (FBS; Microgem Laboratory Research, Milan, Italy), 2 mM L-glutamine, 100 IU/ml penicillin G, and 100 µg/ml streptomycin. Cultures were kept in a humidified incubator at 37°C with a 5% CO_2 atmosphere. Cancer cells were subcultured and plated in 75 cm^2 dishes every 2 days and were utilized during their exponential phase of growth. Treatments were administered 24 hours after plating.

Cell viability was assessed by measuring the mitochondrial metabolic activity, using the 3-(4,5-dimethylthiazol-2-yl)-2,5-biphenyltetrazolium bromide (MTT) assay, as previously reported [18]. Briefly, cells were seeded into 96-well microplates (1×10^4 cells/well). After 24-hour incubation, the samples were treated with extracts at varying concentrations or with 0.5% DMSO (Sigma-Aldrich, St. Louis, MO, USA) as a control vehicle. After 24 hours, 10 µl of the MTT solution (5 mg/ml) was added to each well in the dark, and plates were further incubated for 3 hours at 37°C under the same culturing conditions. Then, the culture medium was removed, and 100 µl of 0.1 N HCl in isopropanol was added to each well to solubilize the formazan crystals. Finally, the absorbance was measured at a wavelength of 570 nm using a BioTek Synergy H1 microplate reader (Agilent, Santa Clara, CA, USA). Cell viability was expressed as a percentage relative to the untreated cells set as 100%.

2.4. Statistical analysis

All the assays were performed at least three times, and the values obtained were analyzed with the KaleidaGraph program (Synergy, 5.0 version, Adalta, Italy). The kinetic and

inhibition parameters were shown as the mean ± standard error. The statistical significance of both nonlinear and linear data fittings was checked using the correlation coefficient R. For the cell viability, statistical significance was determined using ANOVA, followed by Bonferroni's post hoc test, with significance accepted at $p < 0.05$.

3. RESULTS

3.1. Identification of polyphenols extracted from leaves of Mediterranean forage crops

Plants used in this work, namely *L. ornithopodioides*, *H. coronarium*, *M. sativa*, and *C. intybus*, represent a rich source of polyphenols, whose healthy properties as co-adjutants for treatment of neurodegenerative diseases have been described. The relative four extracts, *Lo*CT, *Hc*CT, *Ms*F, and *Ci*F, were subjected to LC-MS/MS analysis in order to characterize their constituents, using 81 standard polyphenols, comprising 43 phenolic acids and 38 flavonoids (Supplementary Table S1). The chromatograms obtained with the four extracts are shown in Figure 1 and Figure 2, for phenolic acids and flavonoids, respectively. The results obtained from the MRM analysis are reported in Tables 1 and 2 for phenolic acids and flavonoids, respectively. Concerning phenolic acids (Table 1), a great variability in composition, concentration, and distribution across the different plants, emerges from the data. Among the 24 identified phenolic acids, several were consistently detected in all extracts, including *p*-coumaric acid, *m*-coumaric acid acid, ferulic acid, 4-hydroxybenzoic acid, phloretic acid, gentisic acid, salicylic acid, and 3,5-dihydroxybenzoic acid, although their concentrations were below the detection limit in some cases. Other phenolic acids, i.e., gallic acid, 2,3-dihydroxybenzoic acid, sinapic acid, 2,6-dihydroxybenzoic acid, dihydrocaffeic acid, vanillic acid, and 2,4-dihydroxybenzoic acid, were present in *Lo*CT, *Hc*CT, and *Ms*F, whereas chlorogenic acid and caffeic acid were present in *Lo*CT, *Hc*CT, and *Ci*F. On the other hand, hydroferulic acid and rosmarinic acid were found in *Lo*CT and *Hc*CT, whereas catechol, trans-2-hydroxycinnamic acid, nordihydroguaiaretic acid, and caffeic acid-phenethyl ester were identified only in *Lo*CT. Finally, aspirin was detected and quantified only in *Ms*F. An evaluation of the most abundant phenolic acids quantified in the various extracts was also attempted (Table 1). Indeed, except for phloretic acid, whose concentration was not evaluated, 3,5-dihydroxybenzoic acid, ferulic acid, and *m*-coumaric acidseem to be the most represented compounds in *Lo*CT; gallic acid and vanillic acid in *Hc*CT; salicylic acid, vanillic acid, and dihydrocaffeic acid in *Ms*F; chlorogenic acid and caffeic acid in *Ci*F.

Concerning the 25 flavonoids identified in the four extracts (Table 2), also in this case, a great variability in their concentration, composition, and distribution emerges from the data. In particular, quercetin, (+)-catechin, polydatin, kaempferol, baicalein, diosmetin, morin, apigenin, rutin, hesperetin, isoliquiritigenin, biochanin A, and formononetin were identified in all extracts, although their concentration was below the quantification limit in some extracts. Myricetin, (+/-)-naringenin, trans-pterostilbene, and genistein were present in *Lo*CT, *Hc*CT, and *Ms*F, whereas baicalin was present in *Lo*CT, *Ms*F, and *Ci*F. On the other hand, (+)-taxifolin and daidzein were found in extracts from *Lo*CT and *Hc*CT, whereas (–)-epicatechin and acacetin were found in extracts from *Hc*CT and *Ms*F, and hesperidin in *Lo*CT and *Ci*F. Lastly, fisetin was exclusively detected and quantified in *Hc*CT, and (–)-epigallocatechin gallate was detected, but not quantified in *Lo*CT. An evaluation of the most abundant flavonoids quantified in each extract was also attempted (Table 2). Indeed, with the exception of isoliquiritigenin and polydatin, whose concentrations were not evaluated, trans-pterostilbene

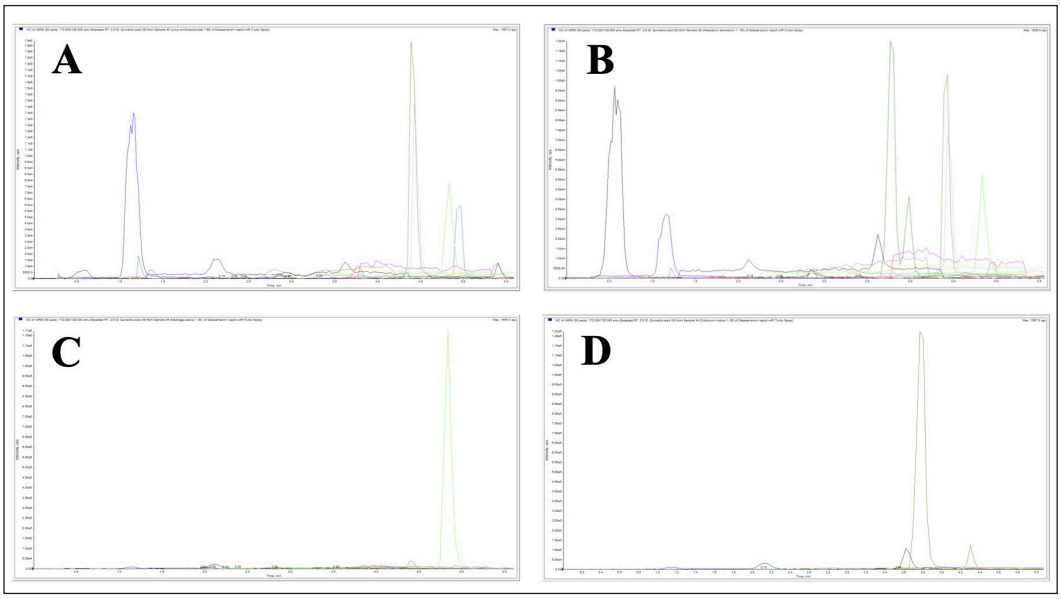

Figure 1. Extract Ion Chromatogram (XIC) of multi reaction monitoring (MRM) of phenolic acids extracted from: A) *Lotus ornithopodioides*, B) *Hedysarum coronarium*, C) *Medicago sativa*, D) *Cichorium intybus*.

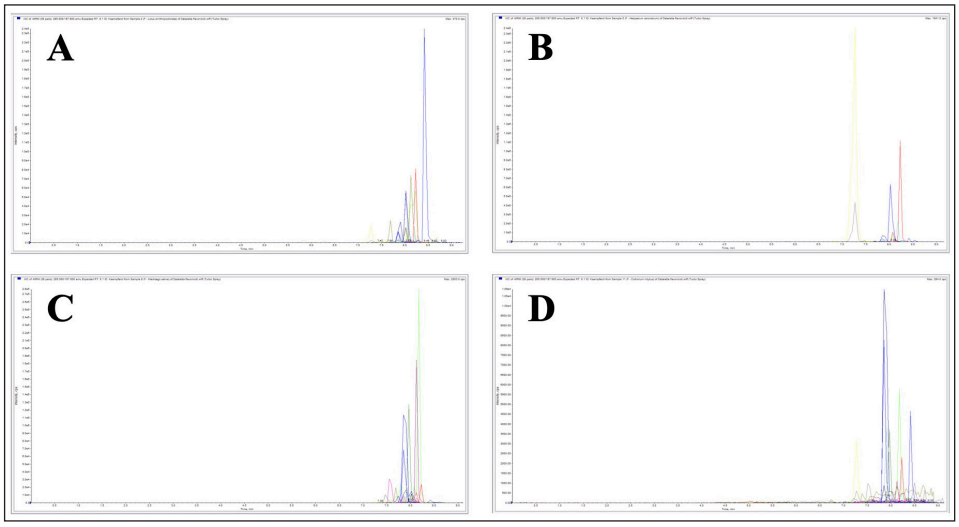

Figure 2. Extract Ion Chromatogram (XIC) of Multi reaction monitoring (MRM) of Flavonoids extracted from: A) *Lotus ornithopodioides*, B) *Hedysarum coronarium*, C) *Medicago sativa*, D) *Cichorium intybus*.

Table 1. Phenolic acids detected in the extracts of *Lotus ornithopodioides*, *Hedysarum coronarium*, *Medicago sativa* and *Cichorium intybus.*

Phenolic acid (µg/ml)	*L. ornithopodioides*	*H. coronarium*	*M. sativa*	*C. intybus*
Gallic acid	<LOD [a]	35.10	<LOD	N/A [b]
Chlorogenic acid	<LOD	9.46	N/A	210.18
Caffeic acid	<LOD	<LOD	N/A	19.65
p-Coumaric acid	1.64	<LOD	<LOD	<LOD
m-Coumaric acid	22.91	11.07	2.45	<LOD
2,3-Dihydroxybenzoic acid	<LOD	<LOD	<LOD	N/A
Ferulic acid	24.24	<LOD	2.28	<LOD
Sinapic acid	3.72	2.73	4.89	N/A
Aspirin	N/A	N/A	4.15	N/A
4-Hydroxybenzoic acid	<LOD	<LOD	<LOD	<LOD
2,6-Dihydroxybenzoic acid	<LOD	<LOD	<LOD	N/A
Dihydrocaffeic acid	<LOD	<LOD	20.33	N/A
Phloretic acid	+ [c]	+	+	+
Hydroferulic acid	<LOD	<LOD	N/A	N/A
Catechol	<LOD	N/A	N/A	N/A
Gentisic acid	<LOD	<LOD	<LOD	<LOD
Salicylic acid	<LOD	<LOD	108.53	<LOD
trans-2-Hydroxycinnamic acid	<LOD	N/A	N/A	N/A
3,5-Dihydroxybenzoic acid	63.53	5.58	<LOD	<LOD
Vanillic acid	1.06	31.86	31.36	N/A
Nordihydroguaiaretic Acid	<LOD	N/A	N/A	N/A
Rosmarinic acid	<LOD	<LOD	N/A	N/A
Caffeic acid phenethyl ester	<LOD	N/A	N/A	N/A
2,4-Dihydroxybenzoic acid	<LOD	<LOD	<LOD	N/A

[a] <LOD, below the Limit of Detection.
[b] N/A, not detected.
[c] +, detected in the extract, but non quantifiable in the selected linearity range.

Table 2. Flavonoids detected in the extracts of *Lotus ornithopodioides*, *Hedysarum coronarium*, *Medicago sativa* and *Cichorium intybus.*

Flavonoid (µg/ml)	*L. ornithopodioides*	*H. coronarium*	*M. sativa*	*C. intybus*
Quercetin	3.18 ± 0.2	28.91 ± 0.5	6.7 ± 0.24	1.81 ± 0.53
(-)-Epicatechin	N/A[a]	1.48 ± 0.12	13.16 ± 0.7	N/A
(+)-Catechin	11.17 ± 0.82	13.15 ± 1.37	24.74 ± 0.93	10.39 ± 0.28
Myricetin	<LOQ[b]	<LOQ	<LOQ	N/A
Polydatin	N/A	+[c]	N/A	+
Kaempferol	7.74 ± 0.09	20.92 ± 3.47	26.17 ± 2.43	3.99 ± 0.97
Acacetin	N/A	4.83 ± 0.42	4.57 ± 0.52	N/A
Baicalein	2.04 ± 0.026	2.72 ± 0.04	2.02 ± 0.03	2.12 ± 0.04
(+)-Taxifolin	<LOQ	<LOQ	N/A	N/A
Diosmetin	3.54 ± 0.09	2.14 ± 0.4	9.54 ± 1	<LOQ
Morin	6.36 ± 1.33	28.42 ± 1.98	2.19 ± 0.09	<LOQ
(-)-Epigallocatechin gallate	<LOQ	N/A	N/A	N/A
(+/-)-Naringenin	1.38 ± 0.08	0.37 ± 0.03	0.83 ± 0.02	N/A
Baicalin	1.86 ± 0.11	N/A	16.01 ± 0.27	1.11 ± 0.02
Hesperidin	23.73 ± 0.08	N/A	N/A	<LOQ
Fisetin	N/A	2.56 ± 0.03	N/A	N/A
Apigenin	2.31 ± 0.03	1.82 ± 0.04	45.42 ± 4.36	1.93 ± 0.03
trans-Pterostilbene	36.33 ± 2.08	775.47 ± 70.45	2.74 ± 0.05	N/A
Rutin	4.6 ± 0.79	771.23 ± 72.12	<LOQ	0.03 ± 0.02
Daidzein	<LOQ	<LOQ	N/A	N/A
Hesperetin	2.4 ± 0.06	3.36 ± 0.39	1.66 ± 0.02	1.47 ± 0.02
Isoliquiritigenin	+	+	+	+
Biochanin A	4.11 ± 0.62	13.67 ± 0.17	2.64 ± 0.18	<LOQ
Formononetin	0.69 ± 0.13	10.02 ± 0.24	0.08 ± 0.03	<LOQ
Genistein	5.1 ± 0.07	7.03 ± 0.17	23.48 ± 0.03	N/A

[a] N/A, not detected; [b] <LOQ, below the Limit of Quantification; [c] +, detected in the extract, but non quantifiable in the selected linearity range.

and hesperidin seem to be the most represented compounds in *Lo*CT; trans-pterostilbene and rutin in *Hc*CT; apigenin, kaempferol, (+)-catechin, and genistein in *Ms*F; (+)-catechin, and kaempferol in *Ci*F.

3.2. Effect of the plant extracts on cholinesterase activity

The effects of *Lo*CT, *Hc*CT, *Ms*F, and *Ci*F on the steady state activity of cholinesterases were investigated. The dose-dependent inhibition profile exerted by the four extracts on AChE and BuChE activity is shown in Figure 3. In the AChE assay (Fig. 3A), a significant and progressive reduction of the steady state activity was observed with *Ms*F, whereas the other extracts were much less effective; indeed, when the extracts were added at 100 µM concentration, the residual AChE activity dropped to nearly 20% with *Ms*F, whereas it remained above 50% with *Lo*CT, *Hc*CT, or *Ci*F. In the BuChE assay (Fig. 3C), the best inhibition profile was observed with *Hc*CT, followed at a distance by *Ms*F, *Lo*CT and *Ci*F, which were much less effective, even when added at 100 µM concentration. These data were also analysed through a logarithmic transformation of the residual activity ratio. The semi-logarithmic plots drawn for AChE (Fig. 3B) and BuChE (Fig. 3D) allowed the extrapolation of the inhibitor concentration that caused a 50% reduction of activity (IC_{50}) through the slope of the resulting linearized inhibition profile. The IC_{50} values reported in Table 3 confirm that, among the four extracts, *Ms*F (52 ± 7 µM) and *Hc*CT (40 ± 6 µM) were endowed with the best inhibition power towards AChE and BuChE, respectively.

To get an insight into the inhibition mechanism of the extracts, kinetic measurements of the AChE activity were realized upon the addition of the various extracts. As shown in Figure 4, their effect was evaluated using both a low, 20–40 µM, and a high, 100 µM, concentration of *Hc*CT, *Ms*F, and *Ci*F; in the case of *Lo*CT, only the high concentration was used, because of the weak inhibition power by this extract. The v_i data of AChE were analyzed in the typical Michaelis–Menten representation (Fig. 4A, 4C, 4E, and 4G) and in Lineweaver–Burk plots (Fig. 4B, 4D, 4F, and 4H), thus allowing the extrapolation of the kinetic parameters K_M and V_{max} in the absence or in the presence of the various plant extracts; the similar values obtained with both Michaelis–Menten and Lineweaver–Burk equations were averaged and reported in Table 4.

Indeed, *Lo*CT produced a decrease in the V_{max} of AChE activity with a minimum increase of the K_M, whereas *Hc*CT caused a progressive decrease of the V_{max} concomitant with some decrease of the K_M. On the other hand, *Ms*F and *Ci*F caused a progressive and consistent increase in the K_M, without apparently affecting the V_{max} of the reaction. On the basis of these effects and using appropriate equations, we calculated the inhibition constant (K_i) of each extract, an important parameter for measuring their inhibition power (Table 4). Indeed, *Ci*F (K_i = 60 ± 8 µM) had the greatest inhibition power, followed by *Ms*F (K_i = 83 ± 12 µM) and *Hc*CT (K_i = 106 ± 14 µM) in order, and at a distance by *Lo*CT (K_i = 239 ± 23 µM). The inhibition mechanism displayed by the extracts was also evaluated by inspecting the intersection of the straight lines obtained in Lineweaver–Burk plots. Indeed, the intersection on the abscissa axis with *Lo*CT (Fig. 4B) suggested a non-competitive inhibition mechanism, whereas the almost parallel lines obtained with *Hc*CT (Fig. 4D) pointed to an uncompetitive mechanism. Vice versa, the

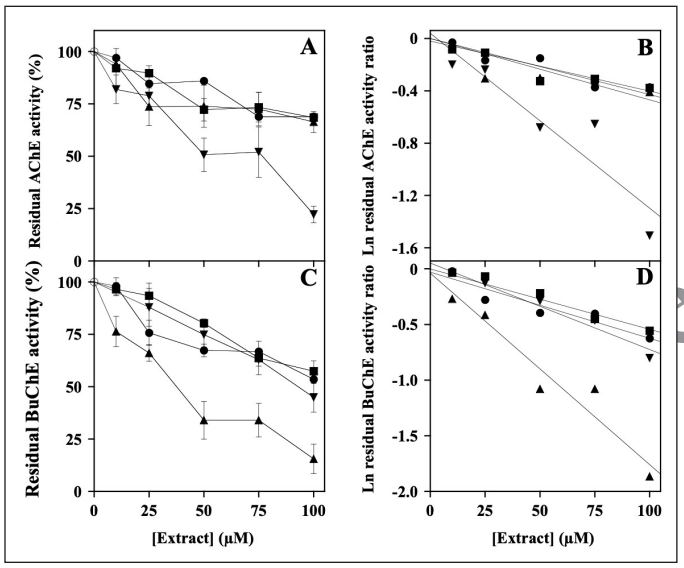

Figure 3. Effect of *Lo*CT, *Hc*CT, *Ms*F and *Ci*F extracts on the steady-state activity of AChE (A,B) and BuChE (C,D). The ratio of activity was assayed in the absence (open circles) or in the presence of the indicated concentrations of *Lo*CT (filled circles), *Hc*CT (triangles), *Ms*F (inverted triangles) and *Ci*F (squares) and expressed as a percentage for AChE (A) and BuChE (C). The data obtained on four or three independent measurements for AChE or BuChE, respectively, were also analyzed after a logarithmic transformation of the activity ratio of AChE (B) and BuChE (D). The correlation coefficient R of the linear equation ranged between 0.909 and 0.964 (B) or 0.977 and 0.990 (D).

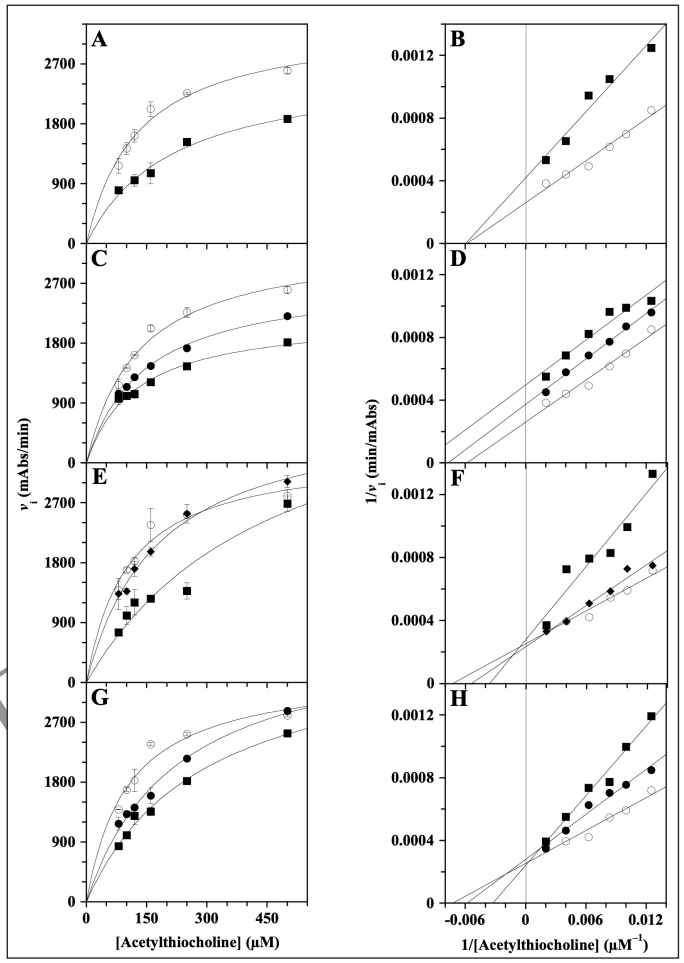

Figure 4. Kinetic analysis of the AChE inhibition by *Lo*CT, *Hc*CT, *Ms*F and *Ci*F extracts. The kinetic measurements of AChE activity were realized as reported in the Methods section in the presence of 80–500 M acetylthiocholine concentration (three determinations for each concentration), without (open circles) or with the following concentrations of polyphenolic extracts: (A, B) 100 µM (squares) *Lo*CT; (C, D) 20 µM (filled circles) or 100 M (squares) *Hc*CT; (E, F) 40 µM (rhombuses) or 100 µM (squares) *Ms*F; (G, H) 20 µM (filled circles) or 100 µM (squares) *Ci*F. Data were reported as the initial velocity of substrate transformation (v_i, mean value ± S.E.) using the hyperbolic Michaelis-Menten equation (A, C, E, G) or the Lineweaver-Burk representation (B, D, F, H). The correlation coefficient R of the hyperbolic or linear equation ranged between 0.978 and 0.987 (A, B), 0.969 and 0.997 (C, D), 0.956 and 0.993 (E, F), 0.968 and 0.994 (G, H).

Table 3. Inhibition by polyphenolic extracts on the steady state activity of cholinesterases.

Extract	Acetylcholinesterase (AChE)		Butyrylcholinesterase (BuChE)	
	Concentration interval (µM)	IC_{50} (µM)	Concentration interval (µM)	IC_{50} (µM)
*Lo*CT	0 – 100	> 100 (R = 0.964)	0 – 100	> 100 (R = 0.977)
*Hc*CT	0 – 100	> 100 (R = 0.909)	0 – 100	40 ± 6 (R = 0.988)
*Ms*F	0 – 100	52 ± 7 (R = 0.963)	0 – 100	89 ± 8 (R = 0.990)
*Ci*F	0 – 100	> 100 (R = 0.960)	0 – 100	> 100 (R = 0.982)

The IC_{50} values were extrapolated from a logarithmic transformation of the activity data obtained on four or three independent measurements for AChE or BuChE, respectively. The correlation coefficient R of the straight lines used for calculation is reported in parentheses.

Table 4. Effect of polyphenolic extracts on the kinetic parameters of AChE.

Extract	Concentration (μM)	K_M acetylthiocholine (μM)	V_{max} (mAbs/minute)*	Putative inhibition mechanism	K_i (μM)	Calculation of K_i
None		134 ± 14	3645 ± 133 (n = 8)			
*Lo*CT	100	167 ± 22	2528 ± 154 (n = 3)	non-competitive	239 ± 23	equation (b)
*Hc*CT	20	136 ± 7	2736 ± 67 (n = 4)	uncompetitive	106 ± 14	equations (c)
	100	109 ± 13	2111 ± 105 (n = 4)			
*Ms*F	40	180 ± 3	4182 ± 29 (n = 3)	competitive	83 ± 12	equation (a)
	100	373 ± 99	4265 ± 733 (n = 3)			
*Ci*F	20	197 ± 27	3832 ± 282 (n = 4)	competitive	60 ± 8	equation (a)
	100	296 ± 7	4043 ± 64 (n = 4)			

*Number of replicates are reported in parentheses.

Table 5. Effect of polyphenolic extracts on the kinetic parameters of BuChE.

Extract	Concentration (μM)	K_M butyrylthiocholine (μM)	V_{max} (mAbs/minute)*	Putative inhibition mechanism	K_i (μM)	Calculation of K_i
None		202 ± 4	4324 ± 42 (n = 4)			
*Lo*CT	100	175 ± 19	2623 ± 133 (n = 3)	non-competitive	155 ± 6	equation (b)
*Hc*CT	40	410 ± 37	3996 ± 259 (n = 3)	mixed, approaching competitive	75 ± 13	equation (a)
	100	380 ± 33	2968 ± 173 (n = 3)			
*Ms*F	20	186 ± 32	3314 ± 294 (n = 3)	non-competitive	97 ± 11	equation (b)
	100	181 ± 35	2390 ± 228 (n = 3)			
*Ci*F	100	111 ± 10	2646 ± 83 (n = 3)	uncompetitive	141 ± 7	equations (c)

*Number of replicates are reported in parentheses.

intersection on the ordinate axis with *Ms*F (Fig. 4F) and *Ci*F (Fig. 4H) indicated a competitive inhibition mechanism.

The same kinetic measurements were performed with the BuChE activity, and the results are presented in Figure 5. Also in this case, the v_i data obtained without or with the extracts were analyzed with the Michaelis–Menten (Fig. 5A, 5C, 5E, and 5G) and Lineweaver–Burk (Fig. 5B, 5D, 5F, and 5H) representation. The resulting values of K_M and V_{max} reported in Table 5 suggest that *Lo*CT and *Ms*F provoked a decrease of the V_{max}, without apparently affecting the K_M of the reaction. On the other hand, *Hc*CT provoked a decrease of the V_{max} concomitant to an increase of the K_M, whereas *Ci*F caused a decrease of both V_{max} and K_M of BuChE activity. The corresponding values of K_i calculated for these extracts are reported in Table 5. Indeed, two extracts, namely *Hc*CT (K_i = 75 ± 13 μM) and *Ms*F (K_i = 97 ± 11 μM), were endowed with a moderate inhibition power towards BuChE, whereas *Lo*CT (K_i = 155 ± 6 μM) and *Ci*F (K_i = 141 ± 7 μM) showed a lower inhibition power. The inhibition mechanism was also evaluated through the Lineweaver–Burk plots. Indeed, the intersection of the straight lines on the abscissa axis with *Lo*CT (Fig. 5B) and *Ms*F (Fig. 5F) suggested their non-competitive inhibition mechanism. In the case of *Hc*CT (Fig. 5D), the lines intersected very close to the ordinate axis, thus suggesting a mixed mechanism, with some prevalence to a competitive inhibition. Finally, the almost parallel lines observed with *Ci*F (Fig. 5H) pointed to an uncompetitive mechanism.

3.3. Effect of the plant extracts on self-aggregation of the $A\beta_{1-40}$ peptide and disaggregation of amyloid fibrils

To evaluate the effect of the extracts on amyloidogenesis of the $A\beta_{1-40}$ peptide, we have analyzed if these samples might interfere with the $A\beta_{1-40}$ self-aggregation process, as well as with the disaggregation of preformed amyloid fibrils (Fig. 6). Concerning the self-aggregation process, the $A\beta_{1-40}$ peptide was incubated alone or in the presence of increasing concentration of the extracts and the extent of fibrils formation was reported in Figure 6A. The data clearly show that all four extracts interfered with the amyloid fibril formation process, with *Hc*CT exerting a slightly higher efficacy among the four extracts. After the logarithmic transformation of the amyloid fibril formation ratio, the resulting semi-logarithmic plots (Fig. 6B) allowed the extrapolation of the IC_{50} values for all extracts. This parameter confirmed that *Hc*CT (144 ± 6 μM) was the most effective in interfering with fibrils formation, followed by *Ci*F and *Lo*CT (205 ± 12 μM and 207 ± 10 μM, respectively), and by *Ms*F (364 ± 10 μM) in the order (Table 6).

Then, we moved to evaluate the effects exerted by the extracts on the amyloid disaggregation process (Fig. 6C). In this assay, all the extracts displayed a lower interfering effect compared to that observed in fibrils formation, although with a different order of effectiveness among them. To better address this point, the data were also analysed through the semi-logarithmic plots (Fig. 6D), thus allowing the extrapolation

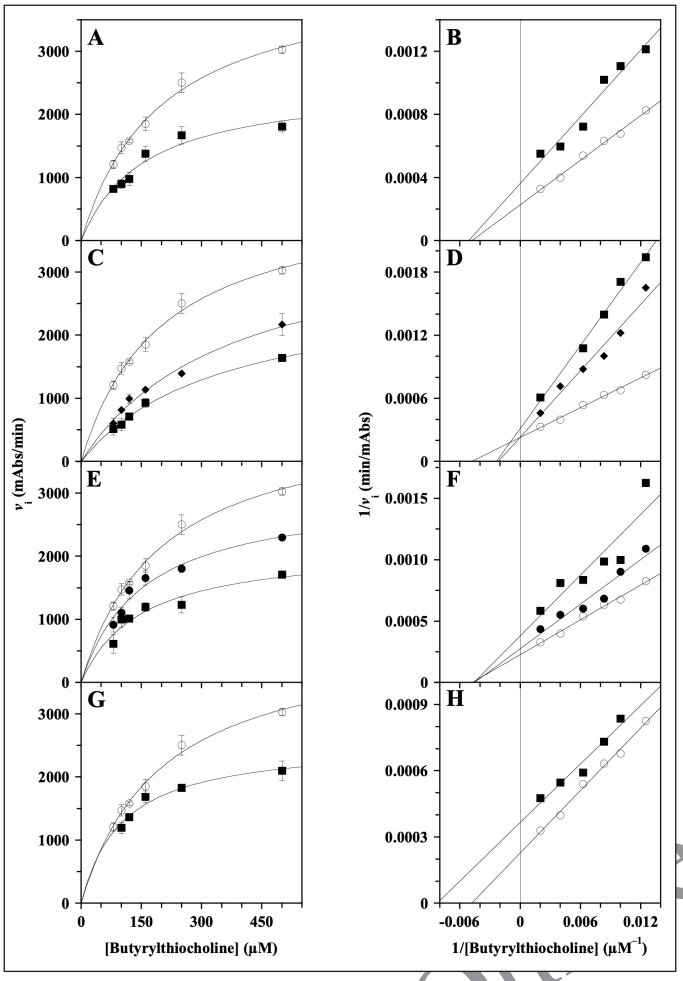

Figure 5. Kinetic analysis of the BuChE inhibition by *Lo*CT, *Hc*CT, *Ms*F and *Ci*F extracts. The kinetic measurements of BuChE activity were realized as reported in the Methods section in the presence of 80–500 μM butyrylthiocholine concentration (three determinations for each concentration), without (open circles) or with the following concentrations of polyphenolic extracts: (A, B) 100 μM (squares) *Lo*CT; (C, D) 40 μM (rhombuses) or 100 M (squares) *Hc*CT; (E, F) 20 μM (filled circles) or 100 μM (squares) *Ms*F; (G, H), 100 μM (squares) CiF. Data were reported as the initial velocity of substrate transformation (v_i, mean value ± S.E.) using the hyperbolic Michaelis-Menten equation (A, C, E, G) or the Lineweaver-Burk representation (B, D, F, H). The correlation coefficient R of the hyperbolic or linear equation ranged between 0.976 and 0.996 (A, B), 0.982 and 0.997 (C, D), 0.907 and 0.996 (E, F), 0.977 and 0.996 (G, H).

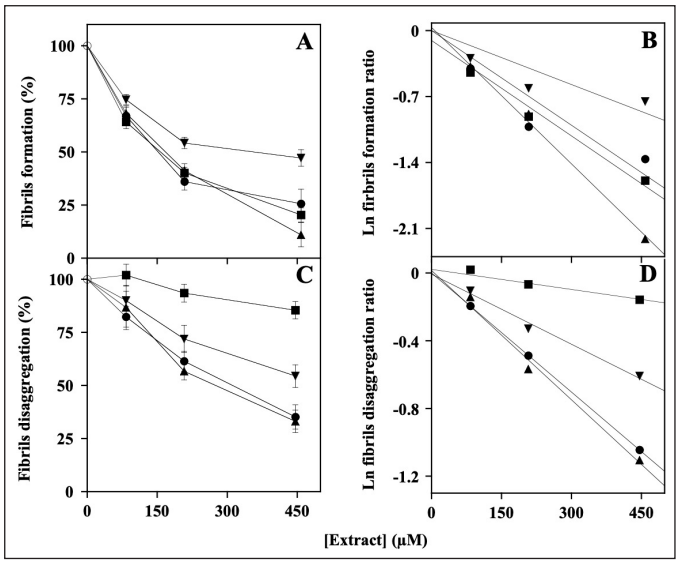

Figure 6. Effect of *Lo*CT, *Hc*CT, *Ms*F and *Ci*F extracts on amyloid fibrils formation (A, B) or disaggregation (C, D) process. The ratio of formation/disaggregation was measured in the absence (open circles) or in the presence of the indicated concentrations of *Lo*CT (filled circles), *Hc*CT (triangles), *Ms*F (inverted triangles) and *Ci*F (squares) and expressed as a percentage for formation (A) or disaggregation (C). The data of three independent measurements for fibril formation or disaggregation, respectively, were also analyzed after a logarithmic transformation of the formation ratio (B) or disaggregation ratio (D). The correlation coefficient R of the linear equation ranged between 0.936 and 0.999 (B) or 0.980 and 1.000 (D).

Table 6. Effect of polyphenolic extracts on the amyloid fibril aggregation and disaggregation process.

Extract	Self-aggregation of $A\beta_{1-40}$ peptide		Disaggregation of $A\beta_{1-40}$ peptide	
	Concentration range (μM)	IC_{50} (μM)	Concentration range (μM)	IC_{50} (μM)
*Lo*CT	0 – 450	207 ± 10 (R = 0.962)	0 – 450	296 ± 12 (R = 1)
*Hc*CT	0 – 450	144 ± 6 (R = 0.999)	0 – 450	272 ± 16 (R = 0.998)
*Ms*F	0 – 450	364 ± 10 (R = 0.936)	0 – 450	502 ± 35 (R = 0.998)
*Ci*F	0 – 450	205 ± 12 (R = 0.995)	0 – 450	> 600 (R = 0.980)

The IC_{50} values were extrapolated from a logarithmic transformation of the data on formation (n = 3) or disaggregation of fibrils (n = 3). The correlation coefficient R of the straight lines used for calculation is reported in parentheses.

of the IC_{50} values reported in Table 6. Indeed, in the fibril disaggregation process, the lowest IC_{50} was found with *Hc*CT (272 ± 16 μM), closely followed by *Lo*CT (296 ± 12 μM), then by *Ms*F (502 ± 35 μM), and at a distance by *Ci*F (> 600 μM).

3.4. Effect of the plant extracts on the viability of a neuroblastoma cell line

The human neuroblastoma SH-SY5Y cell line was chosen to evaluate the effect of the polyphenolic extracts on the cell viability of these cancer cells. To this aim, SH-SY5Y were exposed, for 24-hour treatment, to increasing concentrations of the various extracts up to 250 μM for *Lo*CT, *Hc*CT, and *Ms*F or up to 150 μM for *Ci*F. As a vehicle, the DMSO concentration, was kept always lower than 0.6% (v/v). Cell viability was evaluated with the MTT assay, and the results were reported in Figure 7. The greatest effect was observed with *Ms*F, with an evident dose-dependent reduction of cell viability (Fig. 7C). In particular, after treatment with 250 μM *Ms*F, the cell viability of SH-SY5Y was reduced to 29%. The other extracts were much less effective, and none of them reached a 50% reduction of cell viability, even with the maximum dose of treatment. In particular, cell viability of

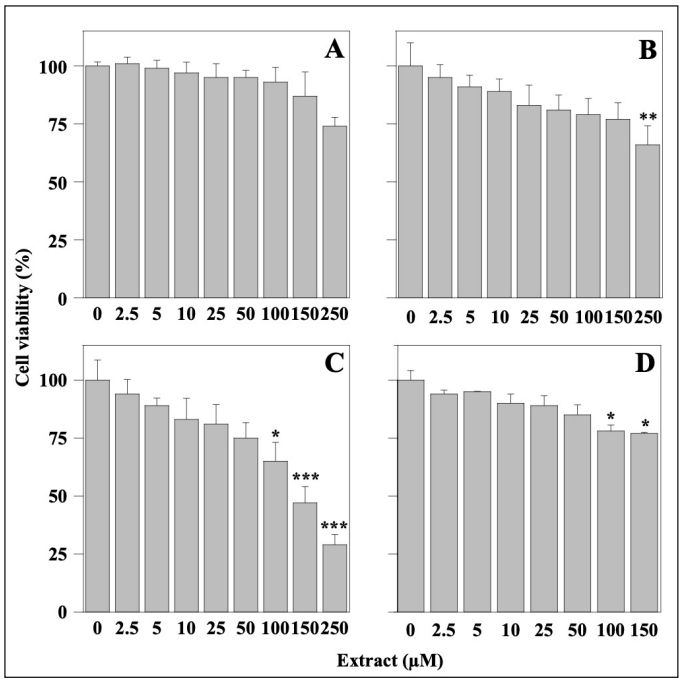

Figure 7. Cell viability of human neuroblastoma SH-SY5Y cell line line after treatment with polyphenolic extracts. Cells were treated for 24 hours with the indicated concentrations of *Lo*CT (panel A), *Hc*CT (panel B), *Ms*F (panel C) or *Ci*F (panel D). Control cells were incubated with 0.6% (v/v) DMSO as a vehicle. Cell viability was determined with the MTT assay, as reported in Materials and Methods. The values, reported as a percentage compared to control cells, represent the mean ± standard error of separate experiments performed in triplicates. The significance was evaluated with $p < 0.05$ (*), 0.01 (**), and 0.001 (***).

SH-SY5Y was reduced to 74%, 66%, or 77%, after treatment with 250 µM *Lo*CT (Fig. 7A), 250 µM *Hc*CT (Fig. 7B), or 150 µM *Ci*F (Fig. 7D), respectively.

4. DISCUSSION

In the last decades, natural polyphenols contained in edible plants have attracted the attention of many researchers for their possible benefits as adjutants of therapies against several human pathologies [36]. Indeed, it is known that an enriched-polyphenol diet is recommended to prevent and alleviate symptoms of neurodegenerative disorders, like AD and PD [37–40]. Polyphenols include a wide variety of different structures, comprising phenolic acids, flavonoids, lignans, and stilbenes; this variety highlights their complex biological functions. Understanding the origin and structural diversity of polyphenolic compounds is crucial for recognizing their antioxidant, anti-inflammatory, and neuroprotective properties.

In a recent paper, we demonstrated that polyphenols extracted from Mediterranean forage crops, such as *L. ornithopodioides*, *H. coronarium*, *M. sativa*, and *C. intybus*, display antioxidant activities, hopefully useful for the design of drugs beneficial for human health [32]. In the present work, the composition of these extracts, namely *Lo*CT, *Hc*CT, *Ms*F, and *Ci*F, was analysed in detail, and the different components, including 24 phenolic acids and 25 flavonoids, were overall identified. The identification of natural compounds in extraction mixtures constitutes an indispensable information for future analysis and focus on the effects of single components on various metabolic pathways. However, at the moment, the working hypothesis followed in the present work is that the effects observed by plant extracts could be due to a specific combination of their various components. Indeed, several dietary regimes, including the popular Mediterranean diet, place at the top the usage of plants as natural foods and/or coadjutants of therapeutic treatments, without considering the effects of each specific component [16,18–21].

Because of the neuroprotective properties possessed by polyphenols [22–24], we decided to investigate on the effects caused by *Lo*CT, *Hc*CT, *Ms*F, and *Ci*F on two crucial enzymes of the neurotransmission process, such as AChE and BuChE. Indeed, all extracts acted as moderate inhibitors of both enzymes with K_i values ranging in the 60–240 µM interval. Among the four samples, the flavonoid-containing extracts had a slightly greater potency towards both cholinesterases, compared to samples containing condensed tannins. *Ms*F had an almost similar inhibition strength against AChE (K_i = 83 µM) and BuChE (K_i = 97 µM), whereas *Ci*F displayed a greater inhibition towards AChE (K_i = 60 µM) compared to BuChE (K_i = 141 µM). On the other hand, despite of their lower strength, extracts with condensed tannins showed a preference for BuChE inhibition, with K_i values of 75 µM and 155 µM for *Hc*CT and *Lo*CT, respectively. The study of the effects on kinetic parameters of both cholinesterase activities revealed differences in the inhibition mechanism exerted by extracts, which are of difficult interpretation. For instance, *Ms*F and *Ci*F had the same competitive mechanism towards AChE, whereas they showed different mechanisms towards BuChE, i.e., non-competitive and uncompetitive for *Ms*F and *Ci*F, respectively. This different behavior could be explained by the combination/overlapping of different inhibition mechanisms exhibited by single components in the extracts.

Another parameter considered for evaluating the possible effects of plant extracts on neurodegenerative diseases was the formation and disassembly of amyloid fibrils deriving from the aggregation of $A\beta_{1-40}$ peptide. Our data on the self-aggregation process indicate that all extracts acted as moderate inhibitors of this process, with IC_{50} values ranging in a moderately wide interval, 144–364 µM; indeed, the greatest efficacy found with *Hc*CT was not so distant from that observed with *Ms*F. Concerning the effects on disaggregation of amyloid fibrils, all extracts displayed a common lower efficacy compared to the self-aggregation process. Furthermore, greater differences were found in the interval of IC_{50} values, ranging from 272 µM to > 600 µM. However, among the various extracts, the *Hc*CT sample had the greatest efficacy in both $A\beta_{1-40}$ peptide self-aggregation and disaggregation process. All these results are congruent with recent studies reporting that plant-derived extracts/compounds can protect neuronal cell damage using an *in vitro* model of AD, by interfering with the $A\beta_{1-40}$ peptide aggregation [11,14,41,42], although the Authors underlined the hindering aspects related to the intracellular

bioavailabilty and the capability to cross the ematoencephalic barrier by substances of natural origin.

We have also checked the cytotoxicity against human neuroblastoma cells, as the usage of polyphenols is probably associated with a reduced incidence of several human pathologies [43,44]. Indeed, we have already reported that the extract from *M. sativa* affected the cell viability of the gastric MKN-28 and AGS cancer lines [32]. Under this regard, the neuroblastoma cell line SH-SY5Y, mimicking immature cholinergic neurons [11,45], is frequently used as an *in vitro* model of AD. We have found that *Ms*F significantly reduced the viability of SH-SY5Y cells, a finding potentially useful for considering natural polyphenolic extracts in cancer therapy. However, comparing the cytotoxicity against neuroblastoma cells with the IC_{50} values for enzyme inhibition and amyloidogenesis, the therapeutic window is restricted to a narrow interval, thus limiting the practical application of these Mediterranean forage crop extracts.

5. CONCLUSION

The results reported in this study indicate that, although to a different extent, *L. ornithopodioides*, *H. coronarium, M. sativa*, and *C. intybus* leaf extracts, inhibit AChE and BuChE, and interfere with the peptide $A\beta_{1-40}$ amyloidogenesis process; therefore, they have properties for postulating the usage as adjutants in the treatment of AD. On the other hand, the reduced cell viability caused by *M. sativa* extract in a neuroblastoma cell line, as well as in gastric cancer cell lines [32], suggests its potential use as a coadjutant in anticancer therapies; however, further investigation is required to assess this hypothesis. In particular, the intracellular bioavailability of the extract components, and their ability to cross the ematoencephalic barrier should be investigated, to establish the potential use of these substances in therapies. All these findings strengthen the consideration that polyphenols can serve as models for developing innovative strategies aimed at the prevention of human diseases and enhancing human health [18,22].

6. AUTHOR CONTRIBUTIONS

All authors made substantial contributions to conception and design, acquisition of data, or analysis and interpretation of data; took part in drafting the article or revising it critically for important intellectual content; agreed to submit to the current journal; gave final approval of the version to be published; and agree to be accountable for all aspects of the work. All the authors are eligible to be an author as per the International Committee of Medical Journal Editors (ICMJE) requirements/guidelines.

7. FUNDING

There is no funding to report.

8. CONFLICTS OF INTEREST

The authors report no financial or any other conflicts of interest in this work.

9. ETHICAL APPROVALS

This study does not involve experiments on animals or human subjects.

10. DATA AVAILABILITY

All the data is available with the authors and shall be provided upon request.

11. PUBLISHER'S NOTE

All claims expressed in this article are solely those of the authors and do not necessarily represent those of the publisher, the editors and the reviewers. This journal remains neutral with regard to jurisdictional claims in published institutional affiliation.

12. USE OF ARTIFICIAL INTELLIGENCE (AI)-ASSISTED TECHNOLOGY

The authors declare that they have not used artificial intelligence (AI)-tools for writing and editing of the manuscript, and no images were manipulated using AI.

REFERENCES

1. Zanetti O, Solerte SB, Cantoni F. Life expectancy in Alzheimer's disease (AD). Arch Gerontol Geriatr. 2009;49 (Suppl. 1):237–43. doi: https://doi.org/10.1016/j.archger.2009.09.035
2. Golbe LI, Leyton CE. Life expectancy in Parkinson disease. Neurology. 2018;91:991–2. doi: https://doi.org/10.1212/WNL.0000000000006560
3. Caligiore D, Giocondo F, Silvetti M. The neurodegenerative elderly syndrome (NES) hypothesis: Alzheimer and Parkinson are two faces of the same disease. IBRO Neurosci Rep. 2022;13:330–43. doi: https://doi.org/10.1016/j.ibneur.2022.09.007
4. Chen JJ. Parkinson's disease: health-related quality of life, economic cost, and implications of early treatment. Am J Manag Care. 2010;16 (Suppl):S87–93.
5. del Campo M, Peeters CFW, Johnson ECB, Vermunt L, Hok-A-Hin YS, van Nee M, *et al.* CSF proteome profiling across the Alzheimer's disease spectrum reflects the multifactorial nature of the disease and identifies specific biomarker panels. Nat Aging. 2022;2:1040–53. doi: https://doi.org/10.1038/s43587-022-00300-1
6. Gątarek P, Kałużna-Czaplińska J. Integrated metabolomics and proteomics analysis of plasma lipid metabolism in Parkinson's disease. Expert Rev Proteom. 2024;21:13–25. doi: https://doi.org/10.1080/14789450.2024.2315193
7. Van Bulck M, Sierra-Magro A, Alarcon-Gil J, Perez-Castillo A, Morales-Garcia JA. Novel approaches for the treatment of Alzheimer's and Parkinson's disease. Int J Mol Sci. 2019;20:719. doi: https://doi.org/10.3390/ijms20030719
8. Lane RM, Potkin SG, Enz A. Targeting acetylcholinesterase and butyrylcholinesterase in dementia. Int J Neuropsychopharmacol. 2006;9:101–24. doi: https://doi.org/10.1017/S1461145705005833
9. Schliebs R, Arendt T. The cholinergic system in aging and neuronal degeneration. Behav Brain Res. 2011;221:555–63. doi: https://doi.org/10.1016/j.bbr.2010.11.058
10. Ballard CG, Greig NH, Guillozet-Bongaarts AL, Enz A, Darvesh S. Cholinesterases: roles in the brain during health and disease. Curr Alzheimer Res. 2005;2:307–18. doi: https://doi.org/10.2174/1567205054367838
11. Maiuolo J, Costanzo P, Masullo M, D'Errico A, Nasso R, Bonacci S, *et al.* Hydroxytyrosol-donepezil hybrids play a protective role in an *in vitro* induced Alzheimer's disease model and in neuronal differentiated human SH-SY5Y neuroblastoma cells. Int J Mol Sci. 2023;24:13461. doi: https://doi.org/10.3390/ijms241713461
12. d'Angremont E, Begemann MJH, van Laar T, Sommer IEC. Cholinesterase inhibitors for treatment of psychotic symptoms in Alzheimer disease and Parkinson disease: a meta-analysis. JAMA Neurol. 2023;80:813–23. doi: https://doi.org/10.1001/jamaneurol.2023.1835

13. Azargoonjahromi A. The duality of amyloid-β: its role in normal and Alzheimer's disease states. Mol Brain. 2024;17:44. doi: https://doi.org/10.1186/s13041-024-01118-1
14. Pagano K, Tomaselli S, Molinari H, Ragona L. Natural compounds as inhibitors of Aβ peptide aggregation: chemical requirements and molecular mechanisms. Front Neurosci. 2020;14:619667. doi: https://doi.org/10.3389/fnins.2020.619667
15. Hansen RA, Gartlehner G, Webb AP, Morgan LC, Moore CG, Jonas DE. Efficacy and safety of donepezil, galantamine, and rivastigmine for the treatment of Alzheimer's disease: a systematic review and meta-analysis. Clin Interv Aging. 2008;3:211–25.
16. Kumar A, Tiwari A, Sharma A. Changing paradigm from one target one ligand towards multi-target directed ligand design for key drug targets of Alzheimer disease: an important role of in silico methods in multi-target directed ligands design. Curr Neuropharmacol. 2018;16:726–39. doi: https://doi.org/10.2174/1570159X16666180315141643
17. Campos-Esparza MR, Torres-Ramos MA. Neuroprotection by natural polyphenols: molecular mechanisms. Cent Nerv Syst Agents Med Chem. 2010;10:269–77. doi: https://doi.org/10.2174/187152410793429728
18. Nasso R, Pagliara V, D'Angelo S, Rullo R, Masullo M, Arcone R. *Annurca* apple polyphenol extract affects acetyl-cholinesterase and mono-amine oxidase *in vitro* enzyme activity. Pharmaceuticals (Basel). 2021;14:62. doi: https://doi.org/10.3390/ph14010062
19. Silva RFM, Pogačnik L. Polyphenols from food and natural products: neuroprotection and safety. Antioxidants (Basel). 2020;9:61. doi: https://doi.org/10.3390/antiox9010061
20. Arias-Sánchez RA, Torner L, Fenton Navarro B. Polyphenols and neurodegenerative diseases: potential effects and mechanisms of neuroprotection. Molecules. 2023;28:5415. doi: https://doi.org/10.3390/molecules28145415
21. Ullah A, Munir S, Badshah SL, Khan N, Ghani L, Poulson BG, *et al.* Important flavonoids and their role as a therapeutic agent. Molecules. 2020;25:5243. doi: https://doi.org/10.3390/molecules25225243
22. Arcone R, D'Errico A, Nasso R, Rullo R, Poli A, Di Donato P, *et al.* Inhibition of enzymes involved in neurodegenerative disorders and $A\beta_{1-40}$ aggregation by *Citrus limon* peel polyphenol extract. Molecules. 2023;28:6332. doi: https://doi.org/10.3390/molecules28176332
23. Orhan I, Aslan S, Kartal M, Şener B, Hüsnü Can Başer K. Inhibitory effect of Turkish *Rosmarinus officinalis L.* on acetylcholinesterase and butyrylcholinesterase enzymes. Food Chem. 2008;108:663–668. doi: https://doi.org/10.1016/j.foodchem.2007.11.023
24. de Torre MP, Cavero RY, Calvo MI. Anticholinesterase activity of selected medicinal plants from Navarra region of Spain and a detailed phytochemical investigation of *Origanum vulgare* L. ssp. *vulgare*. Molecules. 2022;27:7100. doi: https://doi.org/10.3390/molecules27207100
25. Tava A, Biazzi E, Ronga D, Pecetti L, Avato P. Biologically active compounds from forage plants. Phytochem Rev. 2022;21:471–501. doi: https://doi.org/10.1007/s11101-021-09779-9
26. Usman M, Khan WR, Yousaf N, Akram S, Murtaza G, Kudus KA, *et al.* Exploring the hytochemicals and anti-cancer potential of the members of *Fabaceae* family: a comprehensive review. Molecules. 2022;27:3863. doi: https://doi.org/10.3390/molecules27123863
27. Burlando B, Pastorino G, Salis A, Damonte G, Clericuzio M, Cornara L. The bioactivity of *Hedysarum coronarium* extracts on skin enzymes and cells correlates with phenolic content. Pharm Biol. 2017;55:1984–91. doi: https://doi.org/10.1080/13880209.2017.1346691
28. Bora KS, Sharma A. Evaluation of antioxidant and cerebroprotective effect of *Medicago sativa* Linn. against ischemia and reperfusion insult. Evid Based Complement Alternat Med. 2011;2011:792167. doi: https://doi.org/10.1093/ecam/neq019
29. Raeeszadeh M, Mortazavi P, Atashin-Sadafi R. The ntioxidant, anti-inflammatory, pathological, and behavioural effects of *Medicago sativa L.* (Alfalfa) extract on brain injury caused by nicotine in male rats. Evid Based Complement Alternat Med. 2021;2021:6694629. doi: https://doi.org/10.1155/2021/6694629
30. Rolnik A, Olas B. The plants of the *Asteraceae* family as agents in the protection of human health. Int J Mol Sci. 2021;22:3009. doi: https://doi.org/10.3390/ijms22063009
31. Perović J, Tumbas Šaponjac V, Kojić J, Krulj J, Moreno DA, García-Viguera C *et al.* Chicory (*Cichorium intybus* L.) as a food ingredient - Nutritional composition, bioactivity, safety, and health claims: a review. Food Chem. 2021;336:127676. doi: https://doi.org/10.1016/j.foodchem.2020.127676
32. Rullo R, Nasso R, D'Errico A, Biazzi E, Tava A, Landi N, *et al*. Effect of polyphenolic extracts from leaves of Mediterranean forage crops of enzymrs involved in the oxidative stress, and useful for alternative cancer treatments. J Appl Pharm Sci. 2025;15:110–20. doi: https://doi.org/10.7324/JAPS.2025.235772
33. Scacco S, Acquaviva S, França Vieira e Silva F, Zhang JH, Lo Muzio L, Corso G, *et al*. Bioactivity and neuroprotective effects of extra virgin olive oil in a mouse model of cerebral ischemia: an *in vitro* and *in vivo* study. Int J Mol Sci. 2025;26:1771–802.
34. Vitale RM, Morace AM, D'Errico A, Ricciardi F, Fusco A, Boccella S, *et al.* Identification of cannabidiolic and cannabigerolic acids as MTDL AChE, BuChE, and BACE-1 inhibitors against Alzheimer's disease by *in silico*, *in vitro*, and *in vivo* studies. Phytother Res. 2025;39:233–45. doi: https://doi.org/10.1002/ptr.8369
35. Rullo R, Cerchia C, Nasso R, Romanelli V, De Vendittis E, Masullo M, *et al.* Novel reversible inhibitors of xanthine oxidase targeting the active site of the enzyme. Antioxidants (Basel). 2023;12:825. doi: https://doi.org/10.3390/antiox12040825
36. Jalouli M, Rahman MA, Biswas P, Rahman H, Harrath AH, Lee I-S, *et al.* Targeting natural antioxidant polyphenols to protect neuroinflammation and neurodegenerative diseases: a comprehensive review. Front Pharmacol. 2025;16:1492517. doi: https://doi.org/10.3389/fphar.2025.1492517
37. Carregosa D, Mota S, Ferreira S, Alves-Dias B, Loncarevic-Vasiljkovic N, Crespo CL, *et al.* Overview of beneficial effects of (poly)phenol metabolites in the context of neurodegenerative diseases on model organisms. Nutrients. 2021;13:2940. doi: https://doi.org/10.3390/nu13092940
38. Spencer JPE. Food for thought: the role of dietary flavonoids in enhancing human memory, learning and neuro-cognitive performance. Proc Nutr Soc. 2008;67:238–52. doi: https://doi.org/10.1017/S0029665108007088
39. Psaltopoulou T, Sergentanis TN, Panagiotakos DB, Sergentanis IN, Kosti R, Scarmeas N. Mediterranean diet, stroke, cognitive impairment and depression: a meta-analysis. Ann Neurol. 2013;74:580–91. doi: https://doi.org/10.1002/ana.23944
40. Mayr HL, Thomas CJ, Tierney AC, Kucianski T, George ES, Ruiz-Canela M, *et al.* Randomization to 6-month Mediterranean diet compared with a low-fat diet leads to improvement in the dietary inflammatory index scores in patients with coronary heart disease: The AUSMED heart trial. Nutr Res. 2018;55:94–107. doi: https://doi.org/10.1016/j.nutres.2018.04.006
41. Li F, Zhan C, Dong X, Wei G. Molecular mechanisms of resveratrol and EGCG in the inhibition of $A\beta_{42}$ aggregation and disruption of $A\beta_{42}$ protofibril: similarities and differences. Phys Chem Chem Phys. 2021;23:18843–54. doi: https://doi.org/10.1039/d1cp01913a
42. Sun Y, Wang X, Zhang X, Li Y, Wang D, Sun F, *et al.* Di-caffeoylquinic acid: a potential inhibitor for amyloid-beta aggregation. J Nat Med. 2024;78:1029–43. doi: https://doi.org/10.1007/s11418-024-01825-y
43. El-Saadony MT, Yang T, Saad AM, Alkafaas SS, Elkafas SS, Eldeeb GS, *et al.* Polyphenols: Chemistry, bioavailability, bioactivity, nutritional aspects and human health benefits: a review. Int J

Biol Macromol. 2024;277:134223. doi: https://doi.org/10.1016/j.ijbiomac.2024.134223
44. Sun S, Liu Z, Lin M, Gao N, Wang X. Polyphenols in health and food processing: antibacterial, anti-inflammatory, and antioxidant insights. Front Nutr. 2024;11:1456730. doi: https://doi.org/10.3389/fnut.2024.1456730
45. Dubey SK, Ram MS, Krishna KV, Saha RN, Singhvi G, Agrawal M, *et al.* Recent expansions on cellular models to uncover the scientific barriers towards drug development for Alzheimer's disease. Cell Mol Neurobiol. 2019;39:181–209. doi: https://doi.org/10.1007/s10571-019-00653-z

How to cite this article:
D'Errico A, Reveglia P, Nasso R, Maugeri A, Masullo M, Arcone R, Lecce L, De Vendittis E, Rullo R. Effects of polyphenolic extracts from Mediterranean forage crops on cholinesterases and amyloid aggregation relevant to neurodegenerative diseases. J Appl Pharm Sci. 2025. Article in Press. http://doi.org/10.7324/JAPS.2026.251960

SUPPLEMENTARY MATERIAL

The supplementary material can be accessed at the link here: [https://japsonline.com/admin/php/uploadss/4716_pdf.pdf]